Spaced functionalization of poly(ionic liquid)s for boosting catalytic conversion of CO_2 into cyclic carbonates

Qianmeng Zhao[a,d], Shaifei Liu[c], Wen Liu[a,b], Mengqian Fu[a,b], Zhenyang Xu[a], Qian Su[a]*, and Weiguo Cheng[a]*

To characterize the structure of P[XC_{12}VIM][Br], NMR, elemental analysis, SEM, and XRD Contact angle, BET characterization were performed.

S1

The characterization results of ^{13}C NMR are shown in Fig S1. Peaks 1, 2, and 3 represent the three carbons on the imidazole, peaks 6 and 7 represent the carbons on the long alkyl chain, and peaks 4 and 5 represent the carbons on the polymer chain after polymerization. The characterization results are consistent with theory. The elemental analysis results are shown in Table S1, which shows that the actual content of N element is basically consistent with the theoretical value. The above characterization proves that the synthesized P[XC_{12}VIM][Br] is consistent with the target structure.

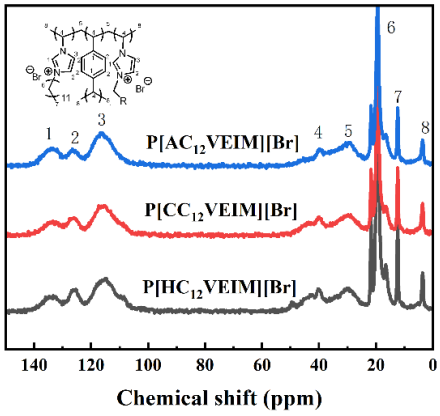

Fig S1 ^{13}C NMR spectrogram of P[XC_{12}VIM][Br]

Table S1 Element analysis of P[XC_{12}VIM][Br] and [VXEIM][Br]

Sample	$N_{calculated\ value}$ (%)	N (%)
[VHEIM][Br]	12.8	14.4
[VCEIM][Br]	11.3	12.1
[VAEIM][Br]	19.3	15.5
P[HC_{12}VIM][Br]	8	7.7
P[CC_{12}VIM][Br]	7.7	7.4
P[AC_{12}VIM][Br]	10.1	7.97

S2

The SEM characterization results of P[XC_{12}VIM][Br] are shown in Fig S2, and it can be seen that all three PILs are block shaped particles formed by particle accumulation, with wrinkled surfaces. The

XRD results of P[XC_{12}VIM][Br] are shown in Fig S3, indicating that P[XC_{12}VIM][Br] has an amorphous structure.

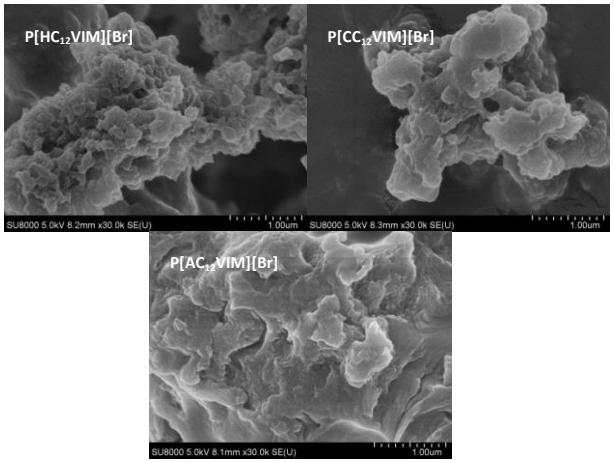

Fig. S2 SEM images of P[XC_{12}VIM][Br]

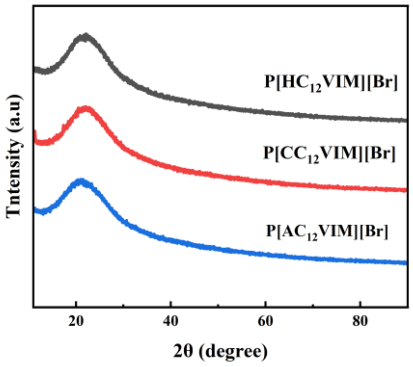

Fig S3 XRD patterns of P[XC_{12}VIM][Br]

S2

The characterization results of the contact angle between P[XC_{12}VIM][Br] and water are shown in Fig S4. It can be seen that the contact angles of the three synthesized PILs are between 110-141°, while the sample without introducing long alkyl chains has almost no contact angle (which is difficult to capture during the testing process). Therefore, the introduction of long alkyl chains can effectively improve the lipophilicity of PILs.

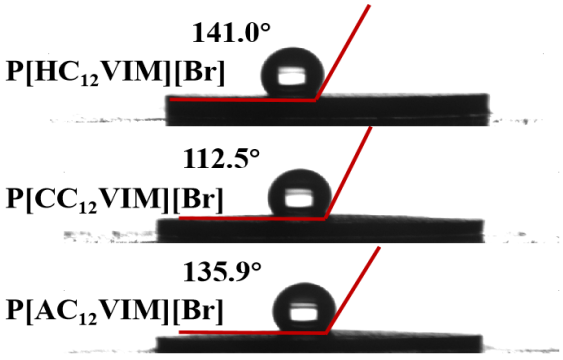

Fig S4 Contact angle of P[XC_{12}VIM][Br] with water

As shown in Table S2, the BET and swelling test results of P[XC_{12}VIM][Br] indicate that only a small amount of large pores are formed by the accumulation of the three PILs. In addition, P[AC_{12}VIM][Br] containing amino groups has the highest swelling performance.

Table S2 N_2 adsorption and desorption results and swelling ratio of P[XC_{12}VIM][Br]

Catalyst	S_{BET} (m^2/g)	Pore Volume (cm^3/g)	Swelling ratio
P[HC_{12}VIM][Br]	4.47	0.011	1.6
P[CC_{12}VIM][Br]	5.92	0.023	1.2
P[AC_{12}VIM][Br]	5.76	0.027	2.1

S3

Product structure characterization:

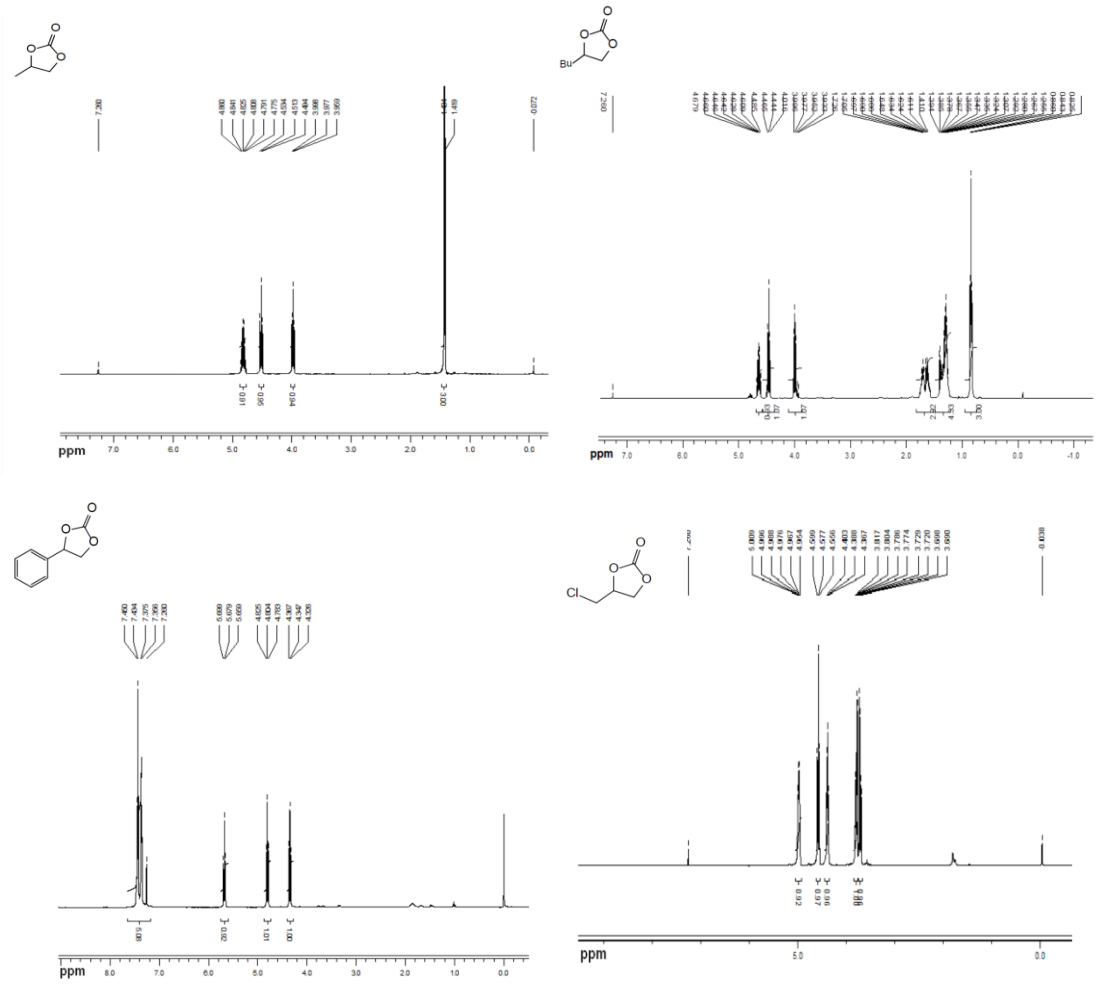

Fig S5 Nuclear magnetic results of different epoxides

S4

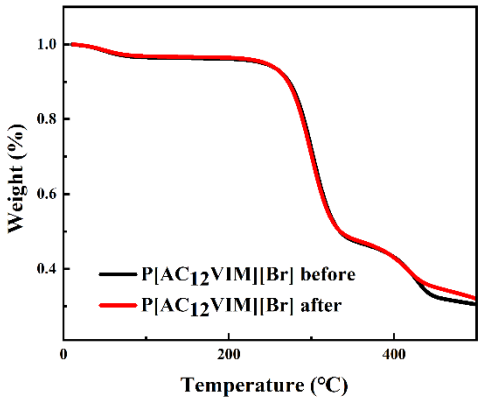

Fig S6 TGA curves of catalysts before and after use